J. Indian Chem. Soc.,
Vol. 93, June 2016, pp. 655-660

Synthesis, characterization and cytotoxicity studies of CuO nanoparticles by using *Gymnema sylvestre* leaf extracts

A. Jafar Ahamed*[a], P. Vijaya Kumar[a], K. Loganathan[a], C. Karthikeyan[b] and A. S. Haja Hameed[b]

[a]P.G. and Research Department of Chemistry, Jamal Mohamed College (Autonomous), Tiruchirappalli-620 020, Tamilnadu, India

E-mail : agjafar@yahoo.co.in

[b]P.G. and Research Department of Physics, Jamal Mohamed College (Autonomous), Tiruchirappalli-620 020, Tamilnadu, India

Manuscript received 05 January 2015, revised 20 May 2016, accepted 25 May 2016

Abstract : *Gymnema sylvestre* leaf extract reduced CuO nanoparticles (NPs) were synthesized successfully by the single step green method. The synthesized NPs retained the monoclinic structure, which was confirmed by X-ray diffraction studies. The TEM image showed the spherical shape morphology with average particle size of 22–30 nm. From the FTIR spectrum the Cu-O stretching frequency was observed at 528 cm^{-1}. The UV-Visible spectrum indicated that the peak at 208 nm confirmed the formation of CuO NPs. The synthesized of CuO NPs exhibited an effective cytotoxic effect against breast cancer cell lines (MCF-7) with an IC_{50} value of 75 µg/ml. The acridine orange (AO) and ethidium bromide (EB) staining results were confirmed the cell death of MCF-7 breast cancer cell line. The toxicological behavior of synthesized CuO NPs was found due to the presence of uneven ridges in morphology and oxygen vacancies.

Keywords : *Gymnema sylvestre,* copper oxide, X-ray diffraction study, cytotoxicity studies, cancer cell line.

Introduction

Nowadays, researchers are focused to prepare the NPs by using plant extracts. Because, it is easily available, ecofriendly, less hazardous, safe to handle and broad range of biomolecules, etc.[1]. CuO is a p type semiconductor with a narrow band gap of 1.2 eV and it has plentiful applications[2]. Borkow *et al.*, reported that CuO NPs inhibit the growth of micro-organisms and used for antiviral properties. For that reason, it has been used in the face makers, wound dressing materials[3]. Recently, the CuO NPs have been synthesized by using different plants such as, *Gloriosa superba*[4], *Carica papaya*[5] and *Cassia alata*[6]. These plant extracts have rich bio-components like alkaloids, flavonoids and terpenoids, which act as a reducing agent to produce nanocrystalline nature of metal and metal oxide NPs in different size and morphology.

Among them *G. sylvestre* belongs to Asclepiadaceae family. It is a traditional Indian medicinal plant used for diabetes mellitus in Siddha and Ayurveda. It is widely used for treatment of asthma, eye complaints and snake bites[7]. This leaf extract contains a large number of bioactive compounds such as alkaloids, flavonoids, phenols, saponins (Gymnemic acid) and tannins[8]. Kantha Devi *et al.*, have reported that Gymnemic acid has been a good reducing agent to prepare the metal oxide nanoparticles[9].

However, to the best of our knowledge, there was no result found in the anticancer activity of *G. sylvestre* reduced CuO NPs against human breast cancer MCF-7 cells. In the present study, we adopt the synthesis of CuO NPs by using *G. sylvestre* leaves extract and their structural and optical characterization studies. Moreover, anticancer activity of CuO NPs was determined against MCF-7 breast cancer cell line.

Experimental

Synthesis of CuO NPs by using G. sylvestre leaves extracts :

In this work, we followed by the previously available literature method[10]. Finely cut *G. sylvestre* leaves (15 g)

were added to 150 ml of double distilled water and boiled at 60 °C for 15 min. The obtained extract was filtered using Whatman No. 1 filter paper and the filtrate was collected in 250 ml Erlenmeyer flask and stored at room temperature for further usage. Thereafter, 0.2 *M* $Cu(NO_3)_2.6H_2O$ solution was added into 150 ml of *G. sylvestre* leaves extract and it was stirred constantly at 80 °C for 6 h. A black color precipitate was obtained. Further the precipitate was dried at 120 °C for 6 h. The obtained CuO nano powder was calcined at 600 °C for 5 h. Thus, CuO NPs were obtained.

Characterization :

The phase purity of the synthesized NPs was determined by X-ray diffractometer (Model : X'PERT PRO PAN analytical). The morphological features of the sample were measured by Transmission electron microscopy (Model : Tecnai F20). The vibrational frequency was measured by Fourier transform infra-red spectroscopy (Perkin-Elmer). The absorption spectrum of the sample was measured on Perkin-Elmer (Lambda 35).

Cell viability assay :

MTT (3-(4,5-dimethylthiazol-2-yl)-2,5-diphenyl tetrazolium bromide) assay was carried out as described in the previously available literature[11]. In brief, the cells were plated separately at a concentration of 1×10^5 cells/well. After 24 h, cells were washed twice with 100 µL of serum-free medium and starved for an hour at 37 °C. After starvation, cells were treated with *G. sylvestre* leaf extracts reduced CuO NPs, in different concentrations (5–100 µg/ml) for 24 h. At the end of the treatment period, the medium was aspirated and serum free medium containing MTT solution [0.5 mg/mL in phosphate-buffered saline (PBS)] was added to each well, and the plates were wrapped with aluminum foil and incubated for 4 h at 37 °C. The MTT containing medium was then discarded and the cells were washed with PBS (200 µL). The crystals were then dissolved by adding 100 µL of DMSO and this was mixed properly by pipetting up and down to each well. Spectrophotometric absorbance of the purple formazan dye was measured in a microplate reader at 570 nm (Biorad 680).

Acridine orange (AO)/Ethidium bromide (EB) staining :

AO/EB staining was performed as described by Spector *et al.*. The cell suspension of each sample containing 5×10^5 cells, was treated with 25 µL of AO and EB solution (3.8 µL of AO and 2.5 µL of EB in PBS) and examined with a fluorescent microscope (Carl Zeiss, Germany) using a UV filter (450–490 nm). Three hundred cells per sample were counted in tetraplicate for each dose point. The cells were scored as viable, apoptotic or necrotic as judged by the staining, nuclear morphology and membrane integrity[12], and the morphological changes were also observed and photographed.

Results and discussion

The formation of CuO NPs was confirmed primarily by the color change from blue to black after 6 h of reaction period. The absorption peak appeared at 208 nm (Fig. 1a) is probably related to the electronic transition between valance band to the conductance band (O 2p → Cu 3d)[13]. Additionally, the plot of photon energy (eV) vs $(\alpha h\nu)^2$ was used to calculate the band gap of the prepared CuO NPs (Fig. 1b). The calculated band gap of CuO NPs was found to be 5.3 eV and it was comparatively higher than bulk value 1.2 eV of CuO.

The X-ray diffraction pattern of synthesized CuO NPs is as shown in Fig. 2a. The XRD peaks are obtained at angles (2θ) of 35.45 and 38.67 corresponding to (002) and (111) planes respectively. Similarly, other peaks are found at angles (2θ) of 32.46, 48.69, 58.19, 61.50 and 67.96 corresponding to (110), (–202), (202), (–113), (–311) and (113) planes of CuO NPs. In order to confirm all the diffraction peaks are indexed as the typical monoclinic structure of CuO NPs (JCPDS data card no : 48-1548) with the C2/c space group. The lattice constants '*a*', '*b*' and '*c*' of CuO NPs can be calculated by using the following relation.

$$\frac{1}{d^2} = \frac{1}{\sin^2\beta}\left(\frac{h^2}{a^2} + \frac{k^2\sin^2\beta}{b^2} + \frac{l^2}{c^2} - \frac{2hl\cos\beta}{ac}\right) \quad (1)$$

The standard lattice constant values of CuO NPs are, a = 4.679 Å, b = 3.431 Å and c = 5.136 Å. In our results, the calculated lattice constant values are, a = 4.6625 Å, b = 3.4255 Å and c = 5.0601 Å. The unit cell volume of the synthesized CuO NPs is calculated by the following relation, $V = abc \sin\beta$. The calculated unit cell volume is 80.8174 Å^3.

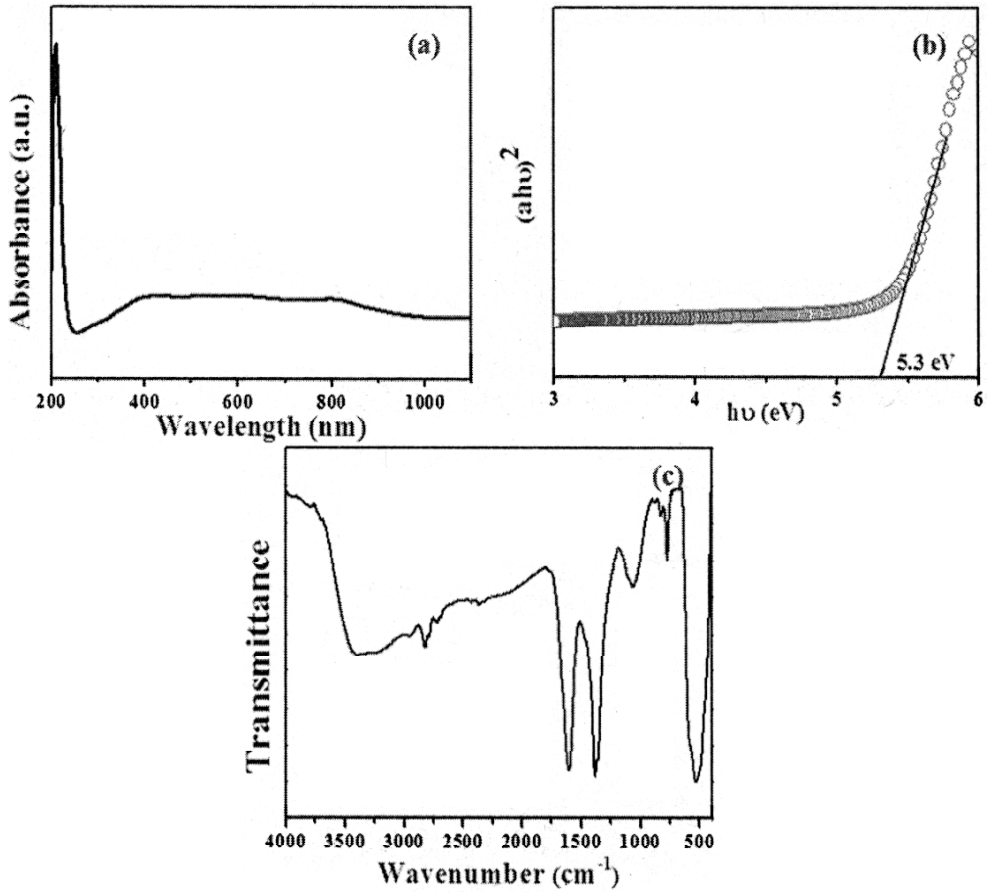


Fig. 1. *G. sylvestre* reduced CuO NPs characterization : (a) UV-Vis spectrum, (b) band gap spectrum and (c) FTIR spectrum.

The average crystallite size of the CuO NPs was calculated by Debye Scherrer's relation.

$$\text{Average crystallite size } (D) = \frac{0.9\,\lambda}{\beta \cos\theta} \qquad (2)$$

where, λ is the wavelength of X-ray used (1.54060 Å), β is the angular peak width at half maximum in radians and θ is Bragg's diffraction angle. The average crystallite size is calculated as 22 nm for CuO NPs.

The TEM image (Fig. 2b) shows that the product consists of spherical shaped particles with particle size ranging from 22 to 30 nm, which is in good agreement with the calculated Debye Scherrer's equation from the XRD pattern. FTIR spectroscopic analysis of *G. sylvestre* reduced CuO NPs is as shown in Fig. 1c. The peak observed at 3430 cm^{-1} is due to O-H stretching. The peak observed at 2816 cm^{-1} is due to symmetric C-H bond. The asymmetric and symmetric vibrations of C=O are observed at 1611 cm^{-1} and 1355 cm^{-1} respectively. The absorption peaks in the range of 879 to 528 cm^{-1} are associated with CuO[14]. The peak appeared at 528 cm^{-1} is due to Cu-O stretching.

Cytotoxicity studies :

The MTT assay was used to evaluate the cytotoxicity of the synthesized CuO NPs on cultured MCF-7 human breast cancer cells by exposing cells for 24 h at various concentrations (5 to 100 µg/ml) as shown in Fig. 2c. In our results, a minimum of 75 µg/ml of *G. Sylvestre* leaf extract reduced CuO NPs is well enough to induce 50% of cell mortality. The main hypotheses for the cytotoxicity are (i) the generation of reactive oxygen species (ROS) such as super oxide anions (O_2^-), hydroxyl radicals ($OH^\bullet$) and hydrogen peroxide (H_2O_2) and (ii) induction of oxidative stress in the cells. The anticancer efficiency of CuO

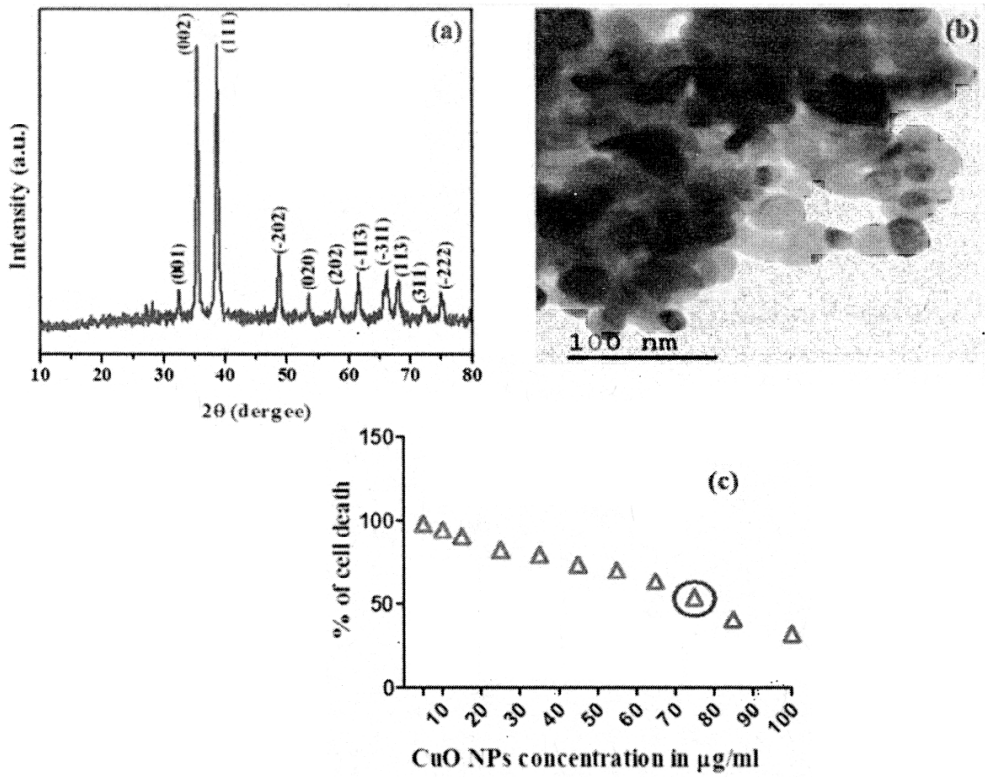


Fig. 2. *G. sylvestre* reduced CuO NPs characterization : (a) XRD pattern, (b) TEM image and (c) MTT assay value *in vitro* cytotoxicity against (MCF-7) human breast cancer cells.

NPs generally depends on their size, morphology, specific surface area, increase in oxygen vacancies, and the diffusion ability of the reactant molecules and the release of Cu^{2+}. When particle size decreases, surface area of the particles increased significantly. It leads to the potential number of chemically reactive oxygen groups on the particle surface that could plays a major role in the adverse biological effects[15]. They can also lead to generation of free radicals after their interaction of cellular compounds, e.g. mitochondrial damage. Another way, ROS is generated through the activation of NADPH-oxidase enzyme which is responsible for O_2^- production in the membrane of phagocytic cells[15]. Generally, NPs with better photocatalytic activity have a large specific surface area and a small crystalline size, which increase oxygen vacancies[16]. Even though, more previous studies have explored the generation of ROS by metal-oxide NPs, few researchers have examined for the electronic properties of metal oxide NPs lead to the key role of ROS generation[17]. The generation of ROS is closely associated with the efficiency of a photocatalyst, depending on the generation rate, the rate of migration, and energy levels of the photoexcited electron hole pairs. In the present study, such enhanced ROS yields may be associated with the electronic properties and microstructure (i.e. grain size, specific surface area and pore, etc.) of the spherical CuO NPs. The electronic structure of the CuO NPs is characterized by the band gap (E_g), which is essentially the energy interval between the valence band (E_v) and the conduction band (E_c), each of which has a high density of states. The synthesized CuO NPs have a higher band gap (E_g) than the incident photon energy (i.e. approximately 5.3 eV) can be photoexcited. Under the UV excitation, electrons are shifted from the valence band to the conduction band, a hole in the valence band was generated simultaneously. The photo excited electrons and holes, then react with an aqueous electron acceptor (i.e. molecular oxygen) and donor (i.e. water and hydroxyl ions) respectively to produce different type of ROS[16].

The generation of highly reactive oxygen species (ROS) such as OH^-, H_2O_2 and O_2^{2-} is explained below. Since

CuO with defects can be activated by both UV and Visible light, electron-hole pairs ($e^- h^+$) can be created. The holes split H_2O molecules (from the suspension of CuO) into OH^- and H^+. Dissolved oxygen molecules are transformed to superoxide radical anions ($^\bullet O_2^-$), which in turn react with H^+ to generate ($HO_2^\bullet$) radicals, which upon subsequent collision with electrons produce hydrogen peroxide anions (HO_2^-). Then, they react with hydrogen ions to produce molecules of H_2O_2. The generated H_2O_2 can penetrate the cell membrane and kill the cancer cells[18,19]. The increased band gap energy revealed from absorption study might be the reason behind our result showing enhanced cytotoxic and oxidation response of CuO NPs in cells[20]. Many researchers are reported that the ROS generation of metal oxide nanoparticles. But the novelty in the present study is that the band gap behaviour of CuO nanoparticles played a major role in the ROS mediated cytotoxicity.

The above mechanism of the light induced generation of ROS can be given as follows.

$$CuO + h\nu \rightarrow e^- + h^+$$

$$h^+ + H_2O \rightarrow {}^\bullet OH + H^+$$

$$e^+ + O_2 \rightarrow {}^\bullet O_2^-$$

$$^\bullet O_2^- + H^+ \rightarrow HO_2^\bullet$$

$$HO_2^\bullet + H^+ + e^- \rightarrow H_2O_2$$

In general, a higher ROS value came from a photocatalyst with a larger surface area and appropriate crystal size, increase the oxygen vacancies and the facilitation of diffusion and mass transportation of reactant molecules. The photocatalytic anticancer mechanism of synthesized CuO NPs was further demonstrated and studied through fluorescence microscopy images. The photocatalytic reactions of CuO NPs are explained above. CuO NPs treated MCF-7 cells after 24 h of visible light irradiation was stained with acridine orange (AO) and ethidium bromide (EB). AO can be yield transported across the membranes of both active and inactive cells, and is then cleaved to yield green fluorescence; on the contrary, EB can enter cells and be cleaved to yield red fluorescence only if cell membranes have been damaged. The fluorescence microscopy images of AO-EB double stained MCF-7 cancer cells are displayed in Fig. 3. Before irradiation, active MCF-7 cells showed bright green fluorescence. There is no apoptosis dead cells are detected in the untreated or control cell (Fig. 3a). It is observed that numbers of orange fluorescence dead cells are detected in 24 h incubation period (Fig. 3b). Under visible light irradiation, ROS produced by the CuO NPs led to the oxidation and subsequent breakdown of membrane lipids, as a result of which EB entered the MCF-7 cells and orange fluorescence was visualized around the cell nuclei. These results indicate that in the oxidative cellular damage process, the cell membranes were partially damaged. This is lead to more generation of ROS production and increased number of oxygen vacancies.

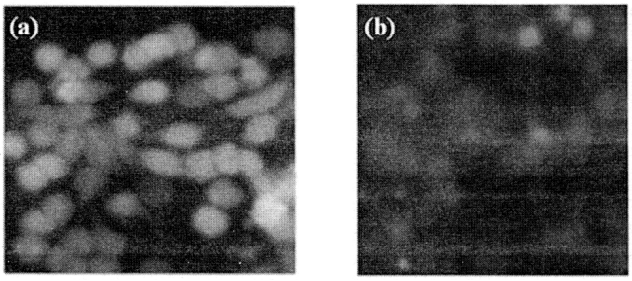


Fig. 3. Fluorescence microscopy images of visible light irradiated AO-EB double stained MCF-7 cells, from live to dead : (a) control and (b) 24 h incubation.

From the XRD results, the crystalline size is found to be 22 nm. Smaller crystal size with a higher surface area leads to higher anticancer activity[18]. The NPs with uneven surface texture due to rough edges[10] and corners contribute to the mechanical damage of the cell membranes of MCF-7 breast cancer cell line[21]. Moreover, TEM image clearly indicated that the CuO NPs have uneven ridges on the outer surface which influence the anticancer activity. Therefore, the combination of various factors such as size, oxygen defects plays a critical role in the toxicological behavior of CuO NPs.

Conclusion

In this study, cost effective CuO NPs has been synthesized by using *G. sylvestre* leaf extract. The XRD studies revealed the formation of monoclinic structure of CuO NPs with a mean size of 22 nm. This smaller crystal size with a higher surface area lead to higher anticancer activity. The TEM image clearly indicated that the CuO NPs possessed spherical shaped size morphology. From the FTIR result, the Cu-O stretching frequency was confirmed

at 528 cm^{-1}. The direct band gap was calculated from the UV-Visible spectrum and it was found to be 5.3 eV. From this higher photocatalytic effect, the oxygen vacancies are found increased. *G. sylvestre* reduced CuO NPs exhibited effective anticancer activity against (MCF-7) breast cancer cell lines with an IC_{50} value of 75 µg/ml for MTT assay. The acridine orange (AO) and ethidium bromide (EB) staining study results, evidenced that the cell death of MCF-7 breast cancer cells. XRD, TEM and UV-Visible spectral evidences support the toxicological behavior of green synthesized CuO NPs, which was found due to small crystallite size with uneven ridges in morphology, crystal defects and increased oxygen vacancies.

References

1. F. Namvar and R. Mohamed, *Materials Letters,* 2014, **116**, 275.
2. K. Mageshwari and R. Sathyamoorthy, *J. Mater. Sci. Technol.,* 2013, **29**, 909.
3. G. Borkow, J. Gabbay, R. Dardik, A. Eidelman, Y. Lavie, Y. Grunfeld, S. Ikher, M. Huszar, R. C. Zatcoff and M. Marikovsky, *Wound Repair Regen,* 2010, **18**, 266.
4. H. Raja Naika, K. Lingaraju, K. Manjunath, Danith Kumar, G. Nagaraju, D. Suresh and H. Nagabhushana, *J. T. Aibah Uni. Sci.,* 2014, **83**, 1.
5. R. Sankar, P. Manikandan, V. Malarvizhi, T. Fathima, S. Shivashangari and V. Ravikumar, *Spectrochimica Acta, Part A : Molecular and Biomolecular Spectroscopy,* 2014, **121**, 746.
6. Jayalakshmi and A. Yogamoorthi, *International Journal of Nanomaterials and Biostructures*, 2014, **4**, 66.
7. T. Dheepakamalini, T. Thiagasundaram, V. Thanigavelan, V. Kaliyamurthi, S. Elansekaran and M. Jegadeesan, *Int. J. Pharm. Phytopharmacol. Res.,* 2012, **2**, 143.
8. Pragya Tiwari, B. N. Mishra, S. Neelam and Sangwan, *Bio-Med Research International,* Article ID 830285, 2014, 1.
9. A. Kantha Devi, A. Lilly Baptista, A. Sathesh Kumar and M. Aarrthy, *Int. J. Nanomedicine*, 2015, **10**, 31.
10. A. Arumugam, C. Karthikeyan, A. S. Haja Hameed, K. Gopinath, S. Gowri and V. Karthika, *Materials Science & Engineering (C)*, 2015, **49**, 408.
11. Maqusood Ahamed and Hisham Alhadlaq, *Onco Targets and Therapy,* 2014, **7**, 269.
12. D. L. Spector, R. D. Goldman and L. A. Leinwand, "Cells : A laboratory manual, culture and Biochemical analysis of cells", Cold Spring Harbor Laboratory Press, New York, 1998, **1**, pp. 34.1-34.9.
13. Neha Topnani, Surendra Kushwaha and Taimur Athar, *International Journal of Green Nanotechnology : Materials Science & Engineering,* 2010, **1**, M67-M73.
14. K. Kannaki, P. S. Ramesh and D. Geetha, *International Journal of Scientific & Engineering Research,* 2012, **3**, 1.
15. Kajal Kumar Dey, Ashutosh Kumar, Rishi Shanker, Alok Dhawan, Meher Wan, Raja Ram Yadav and Avanish Kumar Srivastava, *RSC Advances,* 2012, **2**, 1387.
16. Yang Li, Wen Zhang, Junfeng Niu and Yongsheng Chen, *ACS Nano,* 2012, **6**, 5164.
17. B. Enrico and P. Andrew, *Nanotoxicology,* 2011, **5**, 228.
18. A. S. Haja Hameed, C. Karthikeyan, V. Senthil Kumar, S. Kumaresan and G. Ravi, *J. Mater. Chem. (B),* 2013, **1**, 5950.
19. M. Fang, J. H. Chen, X. L. Xu, P. H. Yang and H. F. Hilder, *Int. Antimicrob. Agents*, 2006, **27**, 513.
20. K. Vijayalakshmi and D. Sivaraj, *RSC Advances,* 2016, **6**, 9663.
21. Xiaolei Wang, Fan Yang, Wen Yangab and Xiurong Yang, *Chem. Commun.*, 2007, 4419.